

# MORPHOLOGY AND MAGNETIC PROPERTIES OF Fe<sub>3</sub>O<sub>4</sub>-ALGINIC ACID NANOCOMPOSITES

## MORFOLOGIJA IN MAGNETNE LASTNOSTI NANOKOMPOZITOV Fe<sub>3</sub>O<sub>4</sub>-ALGINSKA KISLINA

**Małgorzata Kaźmierczak<sup>1,2</sup>, Katarzyna Pogorzelec-Glaser<sup>1</sup>, Andrzej Hilczer<sup>1</sup>,  
Stefan Jurga<sup>2</sup>, Łukasz Majchrzycki<sup>3</sup>, Marek Nowicki<sup>3</sup>, Ryszard Czajka<sup>3</sup>,  
Filip Matelski<sup>3</sup>, Radosław Pankiewicz<sup>4</sup>, Bogusława Łęska<sup>4</sup>, Leszek Kępiński<sup>5</sup>,  
Bartłomiej Andrzejewski<sup>1</sup>**

<sup>1</sup>Institute of Molecular Physics, Polish Academy of Sciences, M. Smoluchowskiego 17, 60179 Poznan, Poland

<sup>2</sup>NanoBioMedical Centre, Adam Mickiewicz University, Umultowska 85, 61614 Poznan, Poland

<sup>3</sup>Poznan University of Technology, Nieszawska 13A, 60965 Poznan, Poland

<sup>4</sup>Faculty of Chemistry, Adam Mickiewicz University, Umultowska 89b, 61614 Poznan, Poland

<sup>5</sup>Institute of Low Temperature and Structure Research, Polish Academy of Sciences, Okolna 2, 50422 Wrocław, Poland  
malgorzata.kaźmierczak@ifmpan.poznan.pl

*Prejem rokopisa – received: 2013-09-27; sprejem za objavo – accepted for publication: 2013-11-19*

The morphology, structure and magnetic properties of the nanocomposites of magnetite (Fe<sub>3</sub>O<sub>4</sub>) nanoparticles and alginic acid (AA) are studied. Magnetite Fe<sub>3</sub>O<sub>4</sub> nanoparticles and the nanoparticles capped with alginic acid exhibit very distinct properties. The chemical bonding between alginic acid and the surface of magnetite nanoparticles results in the recovery of surface magnetization. On the other hand, it also leads to the enhanced surface spin disorder and unconventional behavior of the magnetization observed in Fe<sub>3</sub>O<sub>4</sub>-AA nanocomposites at low temperatures.

Keywords: nanocomposite, magnetite nanoparticles, alginic acid, enhanced magnetization

Preučevali smo morfologijo, strukturo in magnetne lastnosti nanokompozitov na osnovi nanodelcev magnetita (Fe<sub>3</sub>O<sub>4</sub>) in alginske kisline (AA). V primerjavi z magnetitnimi nanodelci izkazujejo nanokompoziti Fe<sub>3</sub>O<sub>4</sub>-alginska kislina precej drugačne lastnosti. Molekule alginske kisline se kemijsko vežejo na površino magnetitnih nanodelcev in s tem povzročijo vrnitev površinske magnetizacije. Hkrati pa se s tem v nanokompozitih Fe<sub>3</sub>O<sub>4</sub>-AA pri nižjih temperaturah poveča površinska neurejenost spinov in nekonvencionalno vedenje magnetizacije.

Ključne besede: nanokompozit, nanodelci magnetita, alginska kislina, povečana magnetizacija

## 1 INTRODUCTION

The interest in the composites of polymers with magnetic nanoparticles stems from their unique physical properties and potential future applications for magnetic-data storage,<sup>1</sup> electronic devices and sensors,<sup>2</sup> biomedical applications in magnetic resonance imaging,<sup>3</sup> drug delivery<sup>4</sup> and hyperthermia agents.<sup>5</sup> From this point of view, one of the most preferred magnetic materials is magnetite Fe<sub>3</sub>O<sub>4</sub> because it is a biocompatible mineral with a low toxicity (for example, the crystals of magnetite are magnetoreceptors in the brains of some animals<sup>6</sup>). It also exhibits a large magnetic moment and a spin-polarized electric current – the features highly desired for the applications in spintronics.

In bulk, magnetite crystallizes in the inverse spinel AB<sub>2</sub>O<sub>4</sub> structure with two nonequivalent Fe sites placed in the *fcc* lattice of O<sup>2-</sup> ions. Tetrahedral A sites contain Fe<sup>2+</sup> ions, whereas octahedral B sites are occupied by Fe<sup>2+</sup> and Fe<sup>3+</sup> ions. The magnetic sublattices located on A and B sites are ferrimagnetically coupled. The mixed valence of Fe ions and fast electron hopping between B sites are responsible for a relatively high electric conductivity of Fe<sub>3</sub>O<sub>4</sub> above the Verwey transition, *T<sub>v</sub>* ≈ 125 K.<sup>7</sup>

Nanostructured magnetite exhibits different magnetic, electronic and optical properties than the bulk material. Particularly, a significant reduction in the magnetization at the surface of Fe<sub>3</sub>O<sub>4</sub> nanoparticles makes them useless for many applications. This obstacle can be overcome by capping the magnetic nanoparticles with polymers<sup>8</sup> or organic acids, which allows a restoration of the surface magnetism.<sup>9</sup>

One of the best capping material is alginic acid, which is a cheap, common and nontoxic natural biopolymer.<sup>10,11</sup> The aim of this work is to study the effect of the alginic-acid capping on the surface magnetization recovery in Fe<sub>3</sub>O<sub>4</sub> nanoparticles.

## 2 EXPERIMENTAL WORK

### 2.1 Sample synthesis

All the chemicals used in the experiments were purchased from SIGMA ALDRICH. To obtain the disaggregated nanoparticles of magnetite Fe<sub>3</sub>O<sub>4</sub>, a portion of 9.0 mmol of FeCl<sub>3</sub> · 6H<sub>2</sub>O was dissolved in 200 mL of ethylene glycol. The solution was vigorously stirred. After 15 min 131.7 mmol of CH<sub>3</sub>COONa and 1.575 mmol of polyethylene glycol PEG 400 were added

and the stirring was continued until they completely dissolved. Then, the solution was transferred into 50 mL teflon reactors and heated using microwave radiation (MARS 5, CEM Corporation) at 160 °C for 25 min. The black suspension of the nanoparticles obtained as a result of the reaction was first cooled, isolated by centrifugation and washed with absolute ethanol. The final product was dried in a vacuum oven at 40 °C. A nanocomposite was prepared from the aqueous dispersion of the magnetite nanopowder and alginic acid (AA) that was then air-dried at room temperature. The nanocomposite had the form of flakes with flat surfaces.

## 2.2 Sample characterization

The crystallographic structures of the samples were studied by means of X-ray powder diffraction (XRD) using an ISO DEBYE FLEX 3000 instrument with a Co lamp ( $\lambda = 0.17928$  nm). The morphology of Fe<sub>3</sub>O<sub>4</sub> nanoparticles was observed using a Philips CM20 SuperTwin transmission electron microscope (TEM). The structures of nanocomposites were studied by means of an atomic force microscope (Dimension Icon®, Bruker) using the magnetic-force-microscope (MFM) mode and NANO-SENSORS™ PPP-MFMR probes. The magnetic measurements were performed using a Quantum Design physical property measurement system (PPMS) fitted with a vibrating-sample-magnetometer (VSM) probe.

## 3 RESULTS AND DISCUSSION

**Figure 1** shows the X-ray powder diffraction patterns of the as-obtained Fe<sub>3</sub>O<sub>4</sub> nanoparticles (panel a) and of the Fe<sub>3</sub>O<sub>4</sub>-AA nanocomposite with the magnetite content equal to the mass fraction  $w = 10\%$  (panel b).

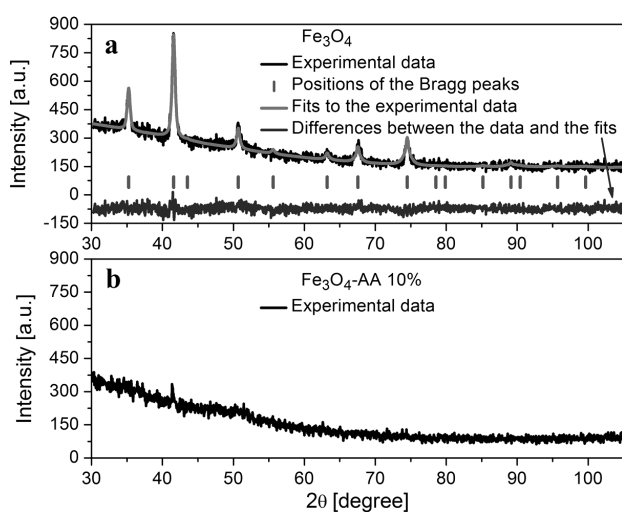


**Figure 1:** XRD powder pattern and line profile fitting of: a) Fe<sub>3</sub>O<sub>4</sub> nanoparticles and b) Fe<sub>3</sub>O<sub>4</sub>-AA nanocomposite

**Slika 1:** XRD-difraktogrami in ujemanje linij za: a) nanodelce Fe<sub>3</sub>O<sub>4</sub> in b) nanokompozit Fe<sub>3</sub>O<sub>4</sub>-AA

The solid line corresponds to the best Rietveld profile fit calculated by means of the FULLPROF software for the cubic crystal structure with the Fd-3m space group and X-ray radiation with the wavelength of 0.17928 nm, as used in the experiment. The vertical bars correspond to the Bragg peaks and the line below them is the difference between the experimental data and the fit. XRD studies verified the Fd-3m point group of the Fe<sub>3</sub>O<sub>4</sub> nanopowder with the lattice parameters of  $a = 0.83641$  nm and the mean crystallite size of 20 nm determined with the Scherrer method. For the composite, the intensity of diffraction peaks is too low to perform an analysis, even if the content of magnetite is high and equal to  $w = 10\%$ .

A TEM image of magnetite nanoparticles is presented in the inset to **Figure 2**. The magnetic nanoparticles are almost monodisperse and spherical. A histogram of the particle-size distribution of Fe<sub>3</sub>O<sub>4</sub> nanoparticles is presented in **Figure 2**. The distribution can be fitted with a log-normal function:

$$f(x) = \frac{1}{x\sqrt{2\pi\sigma^2}} \exp\left[-\frac{1}{2\sigma^2} \ln^2\left(\frac{x}{\langle x \rangle}\right)\right] \quad (1)$$

where  $\langle x \rangle$  is the mean size of the nanoparticles and  $\sigma$  is the distribution width. The values characterizing the distribution are:  $\langle x \rangle = 20.5$  nm and  $\sigma = 0.11$ , with  $\langle x \rangle$  corresponding well to the XRD data.

**Figure 3** shows the topography (panel a), elastic properties (panel b) and magnetic domains (panels c and d) of the Fe<sub>3</sub>O<sub>4</sub>-AA composite surface with the Fe<sub>3</sub>O<sub>4</sub> content of 10%, studied with MFM. The roughness of the surface is below 10 nm for the scanned area of 500 nm × 500 nm. The knobs on the topography image (the white spots) indicate the presence of small agglomerates of Fe<sub>3</sub>O<sub>4</sub> nanoparticles that are also seen as white areas on the phase-contrast image (panel b). The amplitude and phase contrast of the magnetic signal (panels c and d) indicate the presence of magnetic domains with the size close to 100 nm. The actual size of these domains

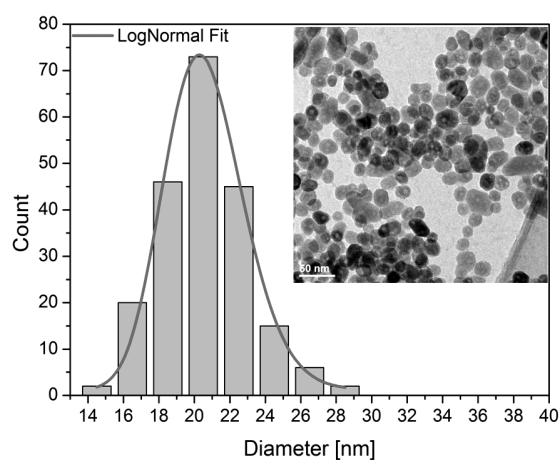


**Figure 2:** Histogram for Fe<sub>3</sub>O<sub>4</sub> nanoparticles with a log-normal fitting. A TEM image is shown in the inset.

**Slika 2:** Histogram nanodelcev Fe<sub>3</sub>O<sub>4</sub>. TEM-posnetek je prikazan v vstavku.

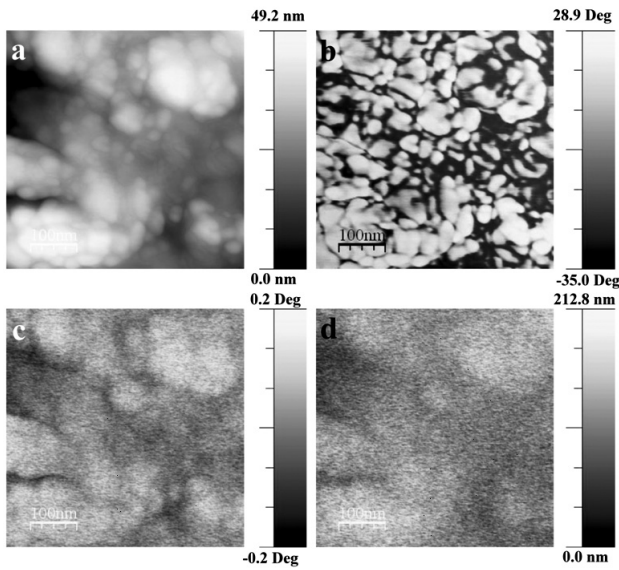


**Figure 3:** a) Surface topography, b) phase contrast, c) magnetic phase and d) magnetic amplitude images for the Fe<sub>3</sub>O<sub>4</sub>-AA composite with the Fe<sub>3</sub>O<sub>4</sub> mass fraction of 10 %

**Slika 3:** a) Površinska topografija, b) fazni kontrast, c) magnetna faza in d) magnetna amplituda kompozitov Fe<sub>3</sub>O<sub>4</sub>-AA z masnim deležem Fe<sub>3</sub>O<sub>4</sub> 10 %

can be smaller than that presented in the figures because of the insufficient spatial resolution of the MFM method (about 50 nm) which causes a smearing of the images.

The results of the magnetic study are presented in **Figures 4** and **5**. The magnetization is normalized with respect to the content of magnetite in the samples. For the nanoparticles of Fe<sub>3</sub>O<sub>4</sub>, the temperature dependence of magnetization  $M \approx T^{1.9}$  deviates from the Bloch law  $M \approx T^{1.5}$  valid for the capped nanoparticles of magnetite (**Figure 4**). The deviation from the Bloch law for the uncapped Fe<sub>3</sub>O<sub>4</sub> nanoparticles can be related to a degraded magnetic ordering at the surface. Moreover, the magnetization of the Fe<sub>3</sub>O<sub>4</sub> nanoparticles at room temperature is only 51 A m<sup>2</sup>/kg, i.e., much below the saturation value for the bulk magnetite ( $\approx 90$  A m<sup>2</sup>/kg), and also lower than the magnetization of the capped particles, equal to 60 A m<sup>2</sup>/kg. The enhancement of the magnetization and the Bloch-like behavior of the capped nanoparticles can be explained in terms of the recovery of surface magnetism due to the chemical bonding between the AA and Fe<sub>3</sub>O<sub>4</sub> nanoparticles. This bonding between the O atoms in the carboxylic groups and two of the four Fe atoms in the Fe-O surface unit cell makes the coordinations and distances close to those in the bulk.<sup>9</sup> The remaining two Fe atoms still exhibit a reduced magnetization because they are closer to the in-plane oxygens, which results in partially empty  $d_x^2 - y^2$  orbitals. The inhomogeneity with respect to the Fe coordination can be responsible for the increased spin disorder or unconventional magnetism at the Fe<sub>3</sub>O<sub>4</sub> surface. This unconventional behavior is manifested as a rapid increase in the magnetization at a low temperature observed for

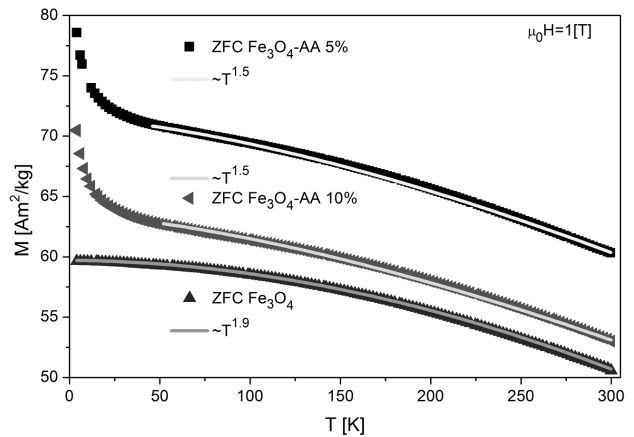


**Figure 4:** Magnetization  $M(T)$  of the Fe<sub>3</sub>O<sub>4</sub> nanoparticles and Fe<sub>3</sub>O<sub>4</sub>-AA composites containing mass fractions 5 % and 10 % of magnetite

**Slika 4:** Magnetizacija  $M(T)$  nanodelcev Fe<sub>3</sub>O<sub>4</sub> in kompozitov Fe<sub>3</sub>O<sub>4</sub>-AA z masnim deležem magnetita 5 % in 10 %

Fe<sub>3</sub>O<sub>4</sub>-AA composites (**Figure 4**). The alternative explanation of this magnetization upturn assumes a quantization of the spin-wave spectrum due to the finite size of the particles that occurs at low temperatures and is responsible for the deviation from the Bloch law.<sup>12</sup>

The magnetization loops  $M(H)$  for the Fe<sub>3</sub>O<sub>4</sub> nanoparticles and Fe<sub>3</sub>O<sub>4</sub>-AA composites are shown in **Figure 5**.

Both the nanoparticles and composites exhibit ferromagnetic (ferrimagnetic) hysteresis loops, which saturate above about 0.3 T. The magnetization of the composites is enhanced as compared to that of the uncapped Fe<sub>3</sub>O<sub>4</sub> nanoparticles. At low temperatures the magnetization loops for the composites are the superpositions of the ferromagnetic and linear contribution from an unconventional magnetism. This unconventional behavior cannot be simply related to the paramagnetism at the degraded

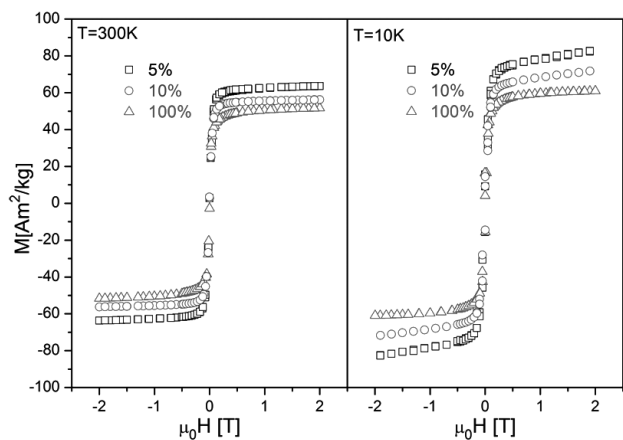


**Figure 5:** Magnetization loops  $M(H)$  for the Fe<sub>3</sub>O<sub>4</sub> nanoparticles and Fe<sub>3</sub>O<sub>4</sub>-AA composites with mass fractions 5 % and 10 % of the magnetite content

**Slika 5:** Histerezna zanka  $M(H)$  nanodelcev Fe<sub>3</sub>O<sub>4</sub> in kompozitov Fe<sub>3</sub>O<sub>4</sub>-AA z masnim deležem magnetita 5 % in 10 %

Fe<sub>3</sub>O<sub>4</sub> surface because it is absent in the uncapped nanoparticles of magnetite.

#### 4 CONCLUSIONS

The capping of Fe<sub>3</sub>O<sub>4</sub> nanoparticles with alginic acid leads to a partial recovery of the surface magnetization. On the other hand, the bonding between alginic acid and Fe<sub>3</sub>O<sub>4</sub> nanoparticles by means of O atoms results in an unconventional magnetism observed at low temperatures.

#### Acknowledgments

This project was supported by the National Science Centre through project No. N N507 229040. M.K. was supported through the European Union – European Social Fund and Human Capital – National Cohesion Strategy. We thank dr. Alja Kupec and dr. Brigita Rožič for the Slovenian translation.

#### 5 REFERENCES

- <sup>1</sup> D. Weller, A. Moser, *IEEE Trans. Magn.*, 35 (1999), 4423
- <sup>2</sup> I. Koh, L. Josephson, *Sensors*, 9 (2009), 8130
- <sup>3</sup> C. W. Jung, P. Jacobs, *Mag. Reson. Imaging*, 13 (1995), 661
- <sup>4</sup> S. Bucak, B. Yavuztürk, A. D. Sezer, *Magnetic Nanoparticles: Synthesis, Surface Modifications and Application in Drug Delivery*, In: A. D. Sezer (ed.), *Recent Advances in Novel Drug Carrier Systems*, InTech Publisher, 2012
- <sup>5</sup> P. Wunderbaldinger, L. Josephson, R. Weissleder, *Bioconjugate Chem.*, 13 (2002), 264
- <sup>6</sup> R. R. Baker, J. G. Mather, J. H. Kennaugh, *Nature*, 301 (1983), 79
- <sup>7</sup> F. Walz, *J. Phys.: Condens. Matter*, 14 (2002), R285
- <sup>8</sup> E. Sówka, M. Leonowicz, B. Andrzejewski, A. D. Pomogailo, G. I. Dzhardimalieva, *J. Alloys Comp.*, 423 (2006), 123
- <sup>9</sup> J. Salafranca, J. Gazquez, N. Pérez, A. Labarta, S. T. Pantelides, S. J. Pennycook, X. Battle, M. Varela, *Nano Letters*, 12 (2012), 2499
- <sup>10</sup> Z. Durmus, H. Sözeri, B. Unal, A. Baykal, R. Topkaya, S. Kazan, M. S. Toprak, *Polyhedron*, 30 (2011), 322
- <sup>11</sup> B. Unal, M. S. Toprak, Z. Durmus, H. Sözeri, A. Baykal, *J. Nanopart. Res.*, 12 (2010), 3039
- <sup>12</sup> K. Mandal, S. Mitra, P. A. Kumar, *Europhys. Lett.*, 75 (2006), 618